Nonlinear decay of foreshock Langmuir waves in the presence of plasma inhomogeneities: Theory and Cluster observations

J. Soucek, V. Krasnoselskikh, Thierry Dudok de Wit, J. Pickett, C. Kletzing

Nonlinear decay of foreshock Langmuir waves in the presence of plasma inhomogeneities: Theory and Cluster observations

J. Soucek,[1,2] V. Krasnoselskikh,[1] T. Dudok de Wit,[1] J. Pickett,[3] and C. Kletzing[3]

[1]   The intense high-frequency electrostatic waves observed in the terrestrial foreshock often have a form of a superposition of two monochromatic waves close to the plasma frequency. We suggest an interpretation of these spectra as signatures of nonlinear decay of Langmuir waves to electron-sound and ion-sound secondary waves. This decay instability is known to have different properties in inhomogeneous plasma, namely the threshold amplitude of this instability is inversely proportional to the scale of the inhomogeneity. We show that the observed dependence of the wave amplitude on the modulation scale of the wave packets is consistent with this property and the theory of absolute decay instability in inhomogeneous plasma can be applied to explain the satellite observations. In this study we used electric field data from the Wide Band Data instrument on board Cluster satellites.

1.   Introduction

[2]   The process of interaction of an electron beam with a homogeneous Maxwellian plasma is relatively well understood from the theoretical point of view. The growth rate of the resultant Langmuir waves is a function of the plasma and beam parameters: beam velocity, beam density, spread of the beam distribution in the velocity space, and a temperature of background plasma. The theory allows for several possible regimes of development and saturation of the beam-plasma instability. In the case of a cold beam, a narrow band wave spectrum is generated and the growth is saturated by trapping of the beam particles by the wave field [*Shapiro*, 1963; *Matsiborko et al.*, 1972]. On the other hand, if the beam is sufficiently warm, the instability generates a wide band spectrum and the action of the wave electric field on particles gives rise to particle diffusion in the velocity space, which decreases the growth rate of the instability to zero. This process is described in the context of quasi-linear theory proposed by *Vedenov et al.* [1961], *Drummond and Pines* [1962], and *Romanov and Filippov* [1961]. The current state of this theory can be found in a recent review by *Shapiro and Sagdeev* [1997]. Yet a different scenario will arise when the wave amplitude overcomes the threshold of the parametric instability, before it is saturated by quasi-linear/trapping processes. In this case a new physical process is involved: the primary Langmuir wave, generated by the beam, decays to a secondary Langmuir wave and an ion-sound wave [*Cairns and Robinson*, 1992]. The decay process transfers the wave energy from the resonant region in the k space to the nonresonant one and the interaction of primary and secondary waves with the particles provides a more efficient dissipation than the quasi-linear process associated with the beam-generated Langmuir wave spectrum only.

[3]   In these theoretical studies, the electron distribution function is assumed to be Maxwellian with an additional beam component (or "bump on tail"). In the case of solar wind, however, the plasma is not strictly Maxwellian but contains two Maxwellian populations of electrons with different temperatures: the cold and hot components [*Feldman et al.*, 1975]. According to recent Ulysses observations [*Maksimovic et al.*, 2000], typical observed values of densities and temperatures of the two electron populations of the solar wind plasma at a distance of 1 AU from the Sun are $n_c = 10$ cm^{-3}, $n_h = 0.6$–0.8 cm^{-3}, $T_c = 10$ eV, $T_h = 100$ eV. This two-temperature plasma allows for propagation of one additional electrostatic wave mode: the electron-sound wave [*Baumjohann and Treumann*, 1996]. This property opens a second channel for the parametric decay instability, where a Langmuir wave decays into electron-sound and ion-sound wave. Comparative study of the two possible channels of the parametric instability can be found in the work of *Hanssen et al.* [1994]. The Cluster observations presented in this paper give a strong evidence that this nonlinear decay is important in the foreshock

---

[1]Laboratoire de Physique and Chimie de l'Environement, CNRS, Orléans, France.

[2]Also at Department of Space Physics, Institute of Atmospheric Physics, Czech Academy of Sciences, Prague, Czech Republic.

[3]Department of Physics and Astronomy, University of Iowa, Iowa City, Iowa, USA.
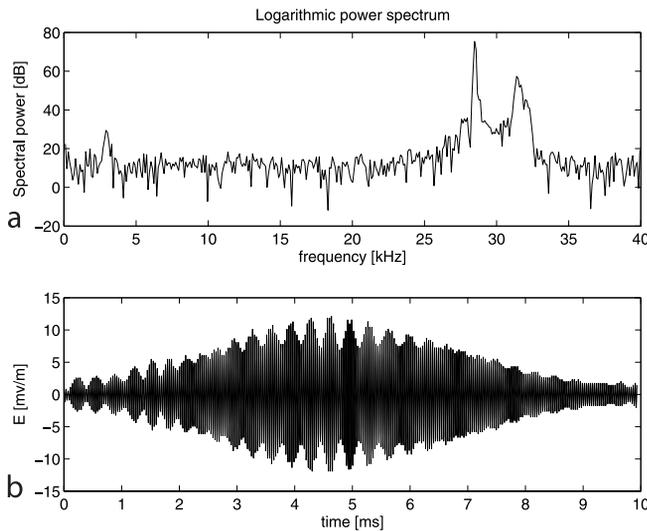
Figure 1. A typical waveform snapshot observed in the foreshock. The two peaks in the spectrum are interpreted as the primary Langmuir wave (larger peak) and a secondary electron-acoustic wave produced by parametric decay.

plasma and we show that the latter case, where an electron-sound wave is generated, is more consistent with the observations.

2. Observations

[4] In this paper, we present an analysis of high-frequency wave observations from the Cluster satellites in the terrestrial foreshock. The WBD (Wide Band Data) instrument [*Gurnett et al.*, 1997] of Cluster captures the electric field waveforms at a sampling frequency of 220 kHz, which is ideally suited to resolve the solar wind Langmuir waves with frequencies close to f_p (usually in the range from 20 to 40 kHz). All data presented here were observed on 17 February 2002, when Cluster was in the foreshock close to the foreshock boundary given by the interplanetary magnetic field line tangent to the bow shock (tangential line). This region of foreshock is appropriate for our study, since Langmuir waves with the largest amplitudes are observed close to this boundary [*Sigsbee et al.*, 2004].

[5] On this day, WBD was operating on three Cluster spacecraft (1, 3, and 4), and on spacecraft 4 the receiver gain was set to the lowest possible level. In this gain-zero mode, the instrument can capture all waves with amplitudes from a few mV/m up to a maximum of 36.9 mV/m, but all lower amplitudes are ignored, being below the digitization threshold. The other two spacecraft were in automatic gain control mode, where the receiver amplification is adjusted according to previously observed amplitudes. In this mode the full dynamic range of the instrument is available, but the probability that the most intense observed waveforms will be clipped due to receiver saturation is higher. The instrument operates in duty cycling mode, where each captured snapshot of 2180 data points (10 ms) is followed by a gap of 69.5 ms.

[6] Since the instrument is using only one dipole antenna placed in the spin plane of the rotating spacecraft, the measured electric field is a projection of the wave electric field on the direction given by immediate antenna orientation. Following the commonly accepted theory of foreshock waves [*Anderson et al.*, 1981], we assume that the observed oscillations are electrostatic waves whose k vectors and electric field vectors are close to parallel to the ambient magnetic field (the angle between k vector and magnetic field is typically less than 15°). This assumption was revised later by *Bale et al.* [1998] using double electric field antenna of Wind. They showed that the intense foreshock waves in fact belong to the z-mode dispersion branch. However, for the range of wave numbers relevant to our study ($kc/\omega > 1$) the z-mode is longitudinally polarized electrostatic wave with a dispersion relation very close to the one of Langmuir waves. In the same article they also show that a majority of these waves is polarized almost parallel to the magnetic field.

[7] Therefore for the purpose of our statistics, we correct the wave amplitude by a factor $1/\cos \alpha$, where α is the angle between the antenna and the mean magnetic field vector. Waveforms captured when this angle was larger than 75° are excluded from the study.

[8] The data set used in the statistical analysis contained 80,459 waveform snapshots observed by spacecraft 1, 3, and 4 during the period from 0700 UT to 1013 UT on 17 February 2002. In this data set were only included waveforms properly represented within the 8-bit digitization range of the instrument whose peak amplitudes exceeded 0.1 mV/m.

[9] Figure 1a presents a typical snapshot of a high-frequency electric field waveform observed by WBD in the foreshock and the corresponding power spectrum. As shown in this example, the envelope of waves in the foreshock is generally structured with characteristic modulation scales of the order of milliseconds [*Bale et al.*, 1997]. Spectral analysis of such waveforms shows that the spectrum frequently consists of two well-pronounced peaks and in many cases, the lower-frequency peak is more intense than the higher-frequency one. We interpret such spectra as a superposition of the primary Langmuir wave and a secondary wave generated by the decay instability as was proposed by *Kellogg et al.* [1996].

[10] The Doppler shift of the peaks in the spectrum in Figure 1 can be exploited to deduce some information on the observed wave modes. The frequency split between the two high-frequency peaks (equal to the frequency of the ion-sound wave peak) is $\Delta f = 2.9$ kHz. Assuming that this split was caused by a Doppler shift of two Langmuir waves with oppositely directed k vectors parallel to the magnetic field, we can calculate the speed of the beam responsible for excitation of the primary wave $v_b = 2f_p V_{sw} \cos \theta / \Delta f$. Substituting the observed values ($v_{SW} = 450$ km/s, $f_p = 30$ kHz, $\theta = 50°$), we obtain a beam energy of 200 eV or $v_b \approx 4 v_{Tc}$, which is significantly lower than a beam energy expected to excite such intense Langmuir waves [*Bale et al.*, 2000]. During our event, the PEACE particle instrument [*Johnstone et al.*, 1997] of Cluster was operating in a low-energy mode, in which it registers only electrons with energies up to 2.6 keV. No beam-like features were observed in this low-energy part of the electron distribution at the same time intervals as the bursts of intense wave activity. The beams associated with the observed waves must therefore lie in the energy range above 2 keV. This is

consistent with previous studies [*Bale et al.*, 2000], where the very intense foreshock waves were found to be correlated with electron fluxes well above 1 keV.

[11] This inconsistency between the magnitude of the Doppler shift and typical beam energies suggests that in a significant number of cases the interpretation in terms of a decay of a Langmuir wave to a Langmuir wave and an ion-sound wave is not applicable. On the contrary, these spectra are perfectly consistent with the second form of the decay, where one of the secondary waves is an electron-acoustic wave. Electron-acoustic waves have significantly larger k vectors than Langmuir waves of the same frequency and the magnitude of the Doppler shift of the secondary wave will therefore be proportionally larger in this case.

[12] Electrostatic foreshock waves are known to be excited by beam-plasma instability triggered by beams of energetic electrons streaming along the background magnetic field. The beam features in the electron distribution were shown to be correlated with the bursts of intense Langmuir [*Anderson et al.*, 1981] and such beams are also observed by the Plasma Electron and Current Experiment (PEACE) instrument of Cluster during the interval studied in this article. The angle of the k vector of the excited wave with respect to the magnetic field is determined by the ratio of the beam thermal velocity to the bulk velocity of the beam. For the observed beam temperatures this angle is usually small (less than 20°) [*Mikhailovskii*, 1974] and the primary waves can be considered to be field-aligned.

[13] The observed high-frequency electric field waves usually exhibit significant modulation on timescales of a few milliseconds. In our analysis, we consider the temporal modulation pattern to be a consequence of spatial structures convected across the spacecraft by the solar wind flow. Assuming that the Langmuir wave under consideration is generated by a 3 keV beam, the group velocity of the waves is approximately 250 km/s and the ion-sound velocity for plasma parameters measured during our event is $C_s \approx$ 80 km/s. Although the Langmuir group velocity is non-negligible (but still smaller) with respect to the solar wind flow velocity (approximately 450 km/s in our case), this assumption still holds if the modulation pattern is dominated by the decay process. In such a case, the envelope of the high-frequency waves is correlated with the ion-sound density perturbations [*Musher et al.*, 1995] and therefore propagates with the ion-sound velocity C_s, which is small compared with the solar wind velocity.

[14] We can thus convert from temporal to spatial scales simply by multiplying the timescales by a flow velocity. This estimate yields spatial modulation scales from several hundred meters to several kilometers. Even though the fastest envelope modulation is in many cases clearly dominated by interference of multiple waves, the slower modulation patterns (several milliseconds to several tens of milliseconds) are representative of the bursty nature of the waves which appear as wave packets with short coherence length. Naturally, the wave packets should be correlated with spatial variations in the electron distribution function (variation of the growth rate of the instability) and in the plasma density (by trapping of waves in density depletions). The plasma inhomogeneities in the free solar wind were found to be mostly isotropic with no preferred direction of elongation [*Celnikier et al.*, 1987]. In the foreshock region,

however, the plasma inhomogeneities are associated with the presence of beams of particles reflected by the shock. The alignment of beams along the magnetic field lines implies that the characteristic scale of plasma parameters variation in the perpendicular direction is smaller than in the parallel direction. Consequently, we expect the amplitude of electrostatic waves to be also modulated more rapidly in the perpendicular direction.

[15] In the context of spacecraft observations, the wave experiments (like WBD) have the necessary time resolution to resolve the small scale changes in wave activity corresponding to the filamentation. Conversely, the sampling rate of the density and plasma composition measurements is usually of the order of seconds, so such a rapid modulation of plasma density cannot be directly observed by these experiments.

3. Model and Interpretation

[16] In the previous section we have shown that the parametric decay of Langmuir waves to electron-sound and ion-sound waves represents a viable interpretation of the observed spectra containing two narrow peaks in the vicinity of the plasma frequency. A minimum threshold value of the wave amplitude $|\vec{E}_0|$ must be reached before the instability can develop. This necessary condition for a plasma with two electron populations can be written as follows:

$$\frac{\epsilon_0 \left| \left(\vec{k}_{es}, \vec{E}_0 \right) \right|^2}{4 n_c M_i C_s^2 k_{es}^2} > \frac{\nu_s \nu_{es}}{\omega_s \omega_{es}}. \tag{1}$$

Here and in the rest of the article, ν_{es} and ν_s are characteristic damping rates of electron-sound and ion-sound waves respectively, n_c, n_h, T_c, T_h are densities and temperatures of cold and hot components of plasma, $\vec{k}_{es}$ is the wave vector of the secondary electron-sound wave and ϵ_0, M_i, m and k_B are the permittivity of vacuum, proton mass, electron mass, and the Boltzmann constant, respectively. The parentheses denote a scalar product of two vectors here and in the rest of the article. The ion-sound velocity C_s in plasma with two electron populations is given by $C_s^2 = k_B (5/3 T_i + T_{eff})/M_i$, where $T_{eff} = (n_c + n_h) T_c T_h / (n_c T_c + n_h T_c)$ [*Hanssen et al.*, 1994].

[17] This process is supposed to be the primary mechanism for saturation of growth of large-amplitude Langmuir waves. Previous studies dedicated to the saturation of wave amplitudes by the decay instability [*Robinson and Cairns*, 1995] revealed that the average observed wave amplitudes are in a good agreement with this interpretation, but they did not address the problem of dynamics of the decaying waves in detail. In this article we show that the saturation amplitudes are dependent on the scale of the modulation. This observation can be explained in two possible ways. The first interpretation is related to the complex dynamics of the system of three interacting waves, whose character depends on the ratio between the increment of the primary wave and characteristic damping of the secondary waves [*Vyshkind and Rabinovich*, 1976; *Alterkop et al.*, 1976; *Hughes and Proctor*, 1990]. The saturation can be reached if the growth rate of the primary wave is smaller than the damping rates

of the secondary waves. However, the stationary points, which are conventionally assumed to determine the wave amplitudes, are in general unstable. This leads to different regimes of dynamic behavior ranging from simple periodic motions to chaotic ones. On the other hand, when the damping of the ion-sound waves becomes large enough, in particular when the ion temperature is comparable with the electron temperature, the dynamic of the system becomes simpler and reduces to quasi-periodic fluctuations of amplitude [*Lefebvre*, 2000] that cannot explain the observed dependence.

[18] Another explanation of the amplitude-scale dependence involves the effect of plasma inhomogeneities on the dynamics of decay instability. Significant inhomogeneities are known to exist in solar wind plasmas, the level of density fluctuations can reach 10% as shown by *Kellogg et al.* [1999].

[19] Hereafter in this section we introduce a mathematical model of growth of Langmuir waves and its saturation due to the decay instability in the inhomogeneous plasma. For the sake of simplicity, we assume the plasma inhomogeneities to have a form of two-dimensional "filaments" elongated with the background magnetic field. The effect of filamentation is taken into account by considering the wave primary wave growth to be confined in these independent spatially decorrelated slabs. Such an approximation allows us to describe the dominant effects, such as the escape of wave energy from the region of growth. The generalization of such model to a plasma with slowly varying parameters is straightforward [*Bers*, 1984]. Let us assume, for simplicity, that the instability is bounded inside a "slab" of finite thickness and let us assume that we can neglect the influence of wave activity that develops around one slab to the activity in the other slab. This allows to consider generation of waves and saturation of their amplitude in each bounded slab independently from the neighboring ones.

[20] Let us fix the coordinate system with the z coordinate parallel to the background magnetic field $\vec{B_0}$ and the x coordinate perpendicular to it. Let L be the width of the slab and let the increment Γ_0 of the linear instability be constant and positive inside the slab $0 < x < L$. Furthermore, let us assume that the saturation of wave amplitudes is completely due to the decay instability of a primary Langmuir wave into an electron-sound wave and an ion-sound wave.

[21] The derivation of the system equations describing the decay instability is described in Appendix A. The resulting equations can be written as follows:

$$\left(\frac{\partial \Psi_0}{\partial t} - \Gamma_0 \Psi_0\right) = -\frac{i\omega_p\left(\vec{k}_0, \vec{k}_{es}\right)}{2k_0^2(n_c + n_h)}\rho_s \Psi_{es} \qquad (2)$$

$$\left(\frac{\partial}{\partial t} + v_{esx}\frac{\partial}{\partial x} + \nu_{es}\right)\Psi_{es} = -\frac{i\omega_{pc}^2\left(\vec{k}_{es}, \vec{k}_0\right)}{2\omega_{es}}\frac{\rho_s^*}{k_{es}^2}\frac{\Psi_0}{n_c} \qquad (3)$$

$$\left(\frac{\partial}{\partial t} + C_{sx}\frac{\partial}{\partial x} + \nu_s\right)\rho_s = -\frac{i\omega_s\omega_p^2\epsilon_0\left(\vec{k}, \vec{k}_0\right)}{2\omega_{es}\omega_L M_i C_s^2}\Psi_0 \Psi_{es}^*. \qquad (4)$$

Here Ψ_0 is the complex amplitude of the perturbation of the electric field potential corresponding to the primarily generated Langmuir wave and $\vec{k}_0$ is its wave vector which is parallel to the z axis. Therefore the group velocity of the primary wave is also parallel to the magnetic field. Ψ_{es} is the amplitude of the perturbation of the electric field potential of a secondary electron sound wave, v_{esx} is the projection of its group velocity to the direction x, and ω_{es}, ν_{es}, and $\vec{k}$ are its frequency, damping rate, and wave vector. In the third equation, ρ_s is the density perturbation of a secondary ion-sound wave, ω_s and ν_s its frequency and damping rate, and $C_{sx} = C_s \sin\theta$ the projection of the ion-sound group velocity to the x direction. Furthermore, the frequencies and wave numbers of the interacting waves must satisfy the resonance conditions

$$\omega_0 = \omega_{es} + \omega_s \ , \ \vec{k}_0 = \vec{k}_{es} + \vec{k}_s. \qquad (5)$$

The dispersion relation of electron sound waves [*Baumjohann and Treumann*, 1996] reads

$$\omega_{es}^2 = \omega_{pc}^2 \frac{k^2\lambda_{Dh}^2}{k^2\lambda_{Dh}^2 + 1}\left(1 + \frac{3T_c}{T_h}\frac{n_h}{n_c} + 3\lambda_{Dc}^2 k^2\right), \qquad (6)$$

where $\lambda_{Dh}^2 = \frac{\epsilon_0 k_B T_h}{n_h e^2}$, $\lambda_{Dc}^2 = \frac{\epsilon_0 k_B T_c}{n_c e^2}$, $\omega_{pc}^2 = \frac{n_c e^2}{\epsilon_0 m}$.

[22] Linear instabilities of Langmuir waves in slab geometry were studied by many authors [*Alekhin et al.*, 1971; *Le Queau et al.*, 1981]. When the amplitude of the primary Langmuir wave exceeds the decay instability threshold, the wave evolution is determined by the energy transfer from the primary wave to the secondary waves and their subsequent damping. However, in our case, where the wave activity is confined in the slab, the instability develops differently than in the homogeneous plasma case described above. Namely, its development is dependent upon the relative velocity of secondary waves across the slab. If the projections of the group velocities to the x axis are oriented in the same direction, the instability will have convective nature. On the other hand, if the projections are oppositely oriented, the instability will become absolute.

[23] An important characteristics of the electron sound waves is their characteristic wavelength, that is larger than the Debye length of cold electron population and shorter than the characteristic Debye length of the hot population. This gives rise to the relation between k vectors of the primary wave and secondary waves: the secondary waves have much larger wave vectors than the Langmuir wave $|\vec{k}_{es}|$, $|\vec{k}_s| \gg |\vec{k}_0|$ and hence $\vec{k}_s \approx -\vec{k}_{es}$. This condition implies that the group velocities of the secondary waves have opposite directions and the decay instability that will develop in the case of the stratified wave activity will be absolute.

[24] The system of equations (2)–(4) should be completed by boundary conditions. We assume without loss of generality, that the wave vector of the x component of the group velocity of the electron sound wave is positive, while the x component of the ion-sound wave group velocity is negative $C_{sx} = -|C_s \sin\theta|$. Here, θ is the angle between the k vector of the secondary ion-sound wave and the magnetic field. When working with equations (2)–(4), we employed an approximation $\omega_p \approx \omega_{es}$ to simplify the expressions.

[25] The problem of stability in the slab is formulated taking the amplitude of the primary wave to be constant inside the slab, and forcing the secondary waves to satisfy the following boundary conditions. The amplitude of the electron sound wave will be equal to zero on the left boundary of the slab $\Psi_{es}(x = 0, t) = 0$ and the ion sound perturbation will be negligible on the right boundary of the slab $\rho_{is}(x = L, t) = 0$. Under these assumptions, we can obtain an additional threshold condition required for the decay instability [*Pesme et al.*, 1973; *Gorbunov*, 1977]:

$$\left[\frac{\epsilon_0 \left| \left(\vec{k}, \vec{E}_0 \right) \right|^2}{4 n_c M_i C_s^2 k^2} \right]^{1/2} > \frac{\pi}{2L} \sqrt{\frac{v_{sx} v_{esx}}{\omega_{es} \omega_s}}. \tag{7}$$

Here $v_{sx} = C_s \sin \theta$ and $v_{esx} = V_{ges} \sin \theta$ are projections of the group velocities of the ion-sound and electron-sound waves on the x direction and L is the characteristic perpendicular scale of the inhomogeneity. Therefore the decay process in a filamented plasma can only proceed if both the condition (1) and the condition (7) are satisfied.

[26] This threshold condition can be rewritten as follows:

$$\left| \vec{E}_0 \right| > \sqrt{\frac{n_c M_i C_s^2}{\epsilon_0}} \frac{\pi}{L} \sqrt{\frac{C_s V_{ges}}{\omega_{es} \omega_s}} \frac{\sin \theta}{\cos \theta}. \tag{8}$$

Substituting the observed plasma parameters to the formulas we obtain a threshold condition

$$\left| \vec{E}_0 \right| > 3.3 \cdot 10^4 \cdot \frac{\tan \theta}{L} \text{ mV/m}. \tag{9}$$

[27] The values of plasma parameters used throughout this paper correspond to the values observed by Cluster on 17 February 2002 in the foreshock: $T_c = 1.4 \cdot 10^5$ K, $T_h \approx 7 \cdot 10^5$ K, $T_i = 4 \cdot 10^5$ K, $n_c = 11 \cdot 10^6$ m^{-3}, $n_h \approx 5.5 \cdot 10^5$ m^{-3}. The density n_c was estimated from the local plasma frequency, T_c was inferred from PEACE [*Johnstone et al.*, 1997] data. Average values obtained by previous observations [*Maksimovic et al.*, 2000] are taken for the hot component properties T_h and n_h.

[28] To understand better the physical meaning of the threshold, one can use an analogy with optical masers. The condition for the growth of the wave energy inside the system is given by the energy balance: the secondary waves must grow fast enough to compensate the energy lost due to escape of waves through the system boundaries. This energy loss can be conveniently characterized by introducing a quality factor of the resonator. When the amplitude of primary wave becomes larger than the instability threshold the growing wave modes are the eigenmodes of the resonator. The following relations hold for the system (2)–(4):

$$\left(\frac{\partial}{\partial t} + 2\nu_{es} \right) \int_0^L \left| \vec{E}_{es}(x) \right|^2 dx + 2 v_{esx} \left| \vec{E}_{es}(L) \right|^2$$

$$= \text{Im} \frac{\omega_{es}}{n_c} \int_0^L \left(\vec{E}_{es}^*(x), \vec{E}_0(x) \right) \rho_s^*(x) dx \tag{10}$$

$$\left(\frac{\partial}{\partial t} + 2\nu_s \right) \int_0^L \left| \rho_s(x) \right|^2 - 2 C_{sx} \left| \rho_s(0) \right|^2$$

$$= \frac{\epsilon_0 \omega_s}{2 M_i C_s^2} \text{Im} \int_0^L \left(\vec{E}_{es}^*(x), \vec{E}_0(x) \right) \rho_s^*(x) \tag{11}$$

Let us introduce the escape factors of the resonator for the electron-sound and the ion-sound waves as follows:

$$\mu_{es} = \frac{2 v_{esx} \left| \rho_{es}(L) \right|^2}{\int_0^L \left| \rho_{es}(x) \right|^2 dx}$$

$$\mu_s = \frac{2 C_{sx} \left| \rho_s(0) \right|^2}{\int_0^L \left| \rho_s(x) \right|^2 dx}.$$

These coefficients characterize the rate of the energy escape from the resonator. If the wave amplitude of electron sound wave has its maximum on the right boundary of the system, the resonator will quickly lose energy through this boundary. Conversely, if the wave amplitude on this boundary is small, the wave mode is trapped inside the resonator and relatively little energy is lost through the boundary and the coefficient μ_{es} is small. The same holds for the ion-sound wave on the left boundary of the resonator.

[29] We can perform some qualitative analysis of the solutions of the system (2)–(4) using the escape factors introduced above. Let us rewrite the system of equations (2)–(4) in the form that includes this effect of the escape of wave energy through the boundaries as an additional damping process characterized by the coefficients μ_{es} and μ_s:

$$\frac{\partial \Psi_0}{\partial t} - \Gamma_0 \Psi_0 = -i \frac{\omega_p}{2} \frac{\left(\vec{k}_0, \vec{k} \right)}{k_0^2} \frac{\rho_s}{n_c + n_h} \Psi_{es}$$

$$\left(\frac{\partial}{\partial t} + \frac{\mu_{es} v_{esx}}{L} + \nu_{es} \right) \Psi_{es} = -\frac{i \omega_{es}}{2} \frac{\left(\vec{k}, \vec{k}_0 \right)}{k^2} \frac{\rho_s^*}{n_c} \Psi_0$$

$$\left(\frac{\partial}{\partial t} + \frac{\mu_s C_{sx}}{L} + \nu_s \right) \rho_s = -i \omega_s \frac{\epsilon_0 \left(\vec{k}, \vec{k}_0 \right) \Psi_0 \Psi_{es}^*}{2 M_i C_s^2}.$$

The stationary solution of this set of equations reads

$$\left| \vec{E}_0 \right|^2 = \frac{4 n_c M_i C_s^2 k_0^2 k^2}{\epsilon_0 \left(\vec{k}, \vec{k}_0 \right)^2} \frac{\left(\frac{\mu_{es} v_{esx}}{L} + \nu_{es} \right) \left(\frac{\mu_s C_{sx}}{L} + \nu_s \right)}{\omega_{es} \omega_s}$$

$$\tag{12}$$

$$\left| \vec{E}_{es} \right|^2 = \frac{4 M_i C_s^2}{\epsilon_0} (n_c + n_h) \frac{\Gamma_0 \left(\frac{\mu_s C_{sx}}{L} + \nu_s \right)}{\omega_p \omega_s} \frac{k_0^2 k^2}{\left(\vec{k}_0, \vec{k} \right)^2}.$$

If we assume that the total damping of electron-sound mode is larger than the growth rate of the primary wave

$(\mu_{es}v_{esx}/L + \nu_{es} \gg \Gamma_0)$, the following condition holds for the wave amplitudes

$$|\vec{E}_0| \gg |\vec{E}_{es}|. \qquad (13)$$

[30] The above stationary solutions can be directly compared with experimental data as they give us the dependence of wave amplitude $|\vec{E}_0|$ (approximated by total observed wave amplitude by virtue of condition (13)) on the size of the resonator L. This scaling law, given by equation (12), reflects the relative importance of different possible mechanisms of energy dissipation. If the dissipation is mainly due to the escape of ion sound and electron sound waves through the boundaries of the resonator, the amplitude-scale dependence is of the form:

$$|\vec{E}_0| \sim \frac{2 \tan\theta}{L} \sqrt{\frac{n_c M_i C_s^2 \mu_s \mu_{es} V_{ges} C_s}{\epsilon_0 \omega_s \omega_{es}}}. \qquad (14)$$

[31] Note that this scaling law differs from the instability threshold formula (9) only by a constant factor $8\sqrt{\mu_s\mu_{es}}/\pi$. If the escape effect is important only for one of the secondary wave modes, while for the second wave mode the damping rate will dominate the dissipation, the wave amplitude will scale as $|\vec{E}_0| \sim L^{-1/2}$. If the damping of waves is the dominant effect for both the ion-sound and electron-sound secondary waves, the saturation amplitude will be independent of the scale.

4. Comparison of Calculated Threshold With Experiment

[32] In this section we investigate the relationship between the characteristic modulation scale of the observed waves and their amplitudes and we compare the experimental results with the theoretical threshold (9). As was described in previous studies [Kellogg et al., 1999] and as can be seen in Figure 1, the vast majority of observed foreshock Langmuir waves is strongly modulated on the timescales of milliseconds. This modulation and the dependence of its characteristic time on wave amplitude was previously studied by Bale et al. [1997]. Our analysis (not presented here) confirms their conclusion that more intense waves are more likely to have slowly varying envelopes while the envelopes of the weaker ones tend to be more patchy and structured.

[33] In our analysis we used a simple direct method to measure the characteristic modulation time. First, the envelope of the wave is estimated using Hilbert transform [Percival and Walden, 1993]. Then we find all minima an maxima of this envelope and we define a characteristic modulation time t_{mod} of each wave packet as the distance between the neighboring minima, under the condition the maximum lying between the minima is sufficiently larger than the larger of the two minima. The amplitude corresponding to this wave packet is defined as the amplitude of the maximum between the minima. In this way, each waveform is divided into multiple wave packets and each wave packet is characterized by its amplitude and width in time. A major experimental limitation for our study is the short length of the waveform snapshot, which allows to study only modulation on timescales well below 10 ms, when the whole wave packet can be captured in the snapshot.

[34] According to the above considerations discussed in section 2, we expect the plasma parameters and wave amplitudes to vary mostly in the direction perpendicular to the background magnetic field and the temporal wave modulation is interpreted as a projection of the spatial perpendicular wave envelope structure convected by the solar wind flow. The spatial modulation scale projected to the B-perpendicular direction is calculated using the formula

$$L_{perp} = t_{mod} \cdot |\vec{V}_p| \cdot \sin\alpha, \qquad (15)$$

where t_{mod} is the characteristic modulation time of the wave packet (defined above), $\vec{V}_p$ is the solar wind velocity vector, and α is the angle between $\vec{V}_p$ and the magnetic field.

[35] To make a direct comparison of data with our model, we need to estimate the width of the slab L. Since we assume that the large amplitude waves are trapped inside the slabs, the width of the slab is equal to the perpendicular width of the trapped wave packet. In a majority of cases, only a fraction of the whole wave packet is observed by WBD because of the 10 ms length of the snapshot. However, in a few cases, like the ones displayed in Figure 2, the full packet is captured. We can conclude from Figure 2 that the eigenmodes trapped inside the slab are typically not the first modes but more likely higher-order modes. Therefore we can estimate the width of the packet as an integer multiple of the characteristic modulation scale estimated as described above. On the basis of observations, we set this multiplier to a fixed value of 10.

[36] Figure 3 shows a joint two-dimensional distribution of the amplitudes of the wave packets versus their perpendicular spatial width. Superimposed on the figure are the theoretical curves of absolute decay instability threshold as a function of the inhomogeneity scale (9) and the amplitude of a stationary solution (14) calculated for a chosen typical values of the parameter $\theta = 15°$.

[37] The comparison of the histogram with the curves shows that a significant number of waves exceeds the threshold for the absolute instability and most of the waveforms lie below the curve of stationary solution amplitudes. Furthermore, the shape of the observed distribution is consistent with the $|\vec{E}_0| \sim 1/L$ dependence of saturated wave amplitudes on the scale. Interpreting this scaling law in terms of the above theory, we conclude that the escape of both ion-sound end electron-sound waves from the resonator is the dominant process responsible for damping of the primary beam-generated wave.

5. Summary and Discussion

[38] In this paper we have shown that the nonlinear decay of Langmuir waves contributes significantly to the dissipation of energy of very intense beam-generated waves in the foreshock. The two-temperature plasma of solar wind allows for two possible channels of the decay instability. One is a decay of Langmuir wave to Langmuir and ion sound waves, the other decay process generates an electron-
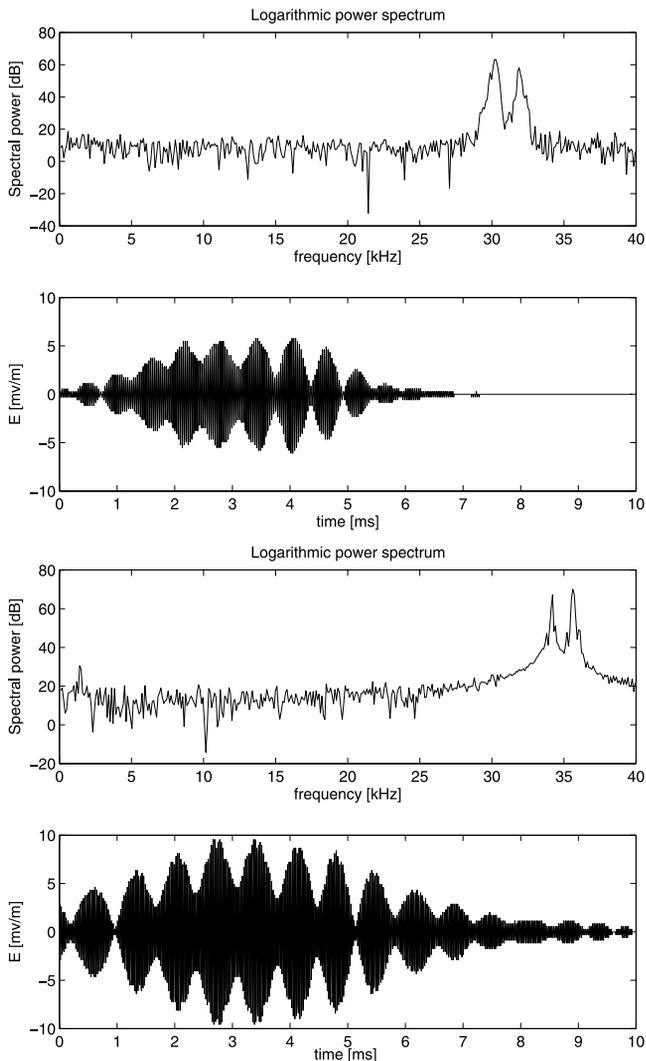
Figure 2. Two examples of waveforms, where the whole wavepacket is contained within the length of the snapshot. The modulation suggests, that the standing wave trapped in the resonator is not the first mode, but has a higher mode number.

parametric instabilities. The presence of inhomogeneities can be responsible for suppression of the Langmuir → Langmuir decay channel as a consequence of a loss of coherency of Langmuir waves. If the coherency length in inhomogeneous plasma becomes comparable with the wavelength of the secondary Langmuir wave, the instability changes its character. In the quasi-homogeneous case, the phases of the waves involved in the decay are dynamically related and coherent, while in the case where the coherency length is comparable to the wavelength, the phases should be considered random. This changes the dynamics of the instability and results in a strong decrease in the instability growth rate [*Laval et al.*, 1976]. Since the electron-sound waves have significantly smaller wavelengths, the electron-sound channel of the decay may still keep the properties of coherent wave interaction, while the Langmuir → Langmuir channel will be affected by the phase randomization.

[40] We proposed a model that describes the decay instability in the presence of plasma inhomogeneities. In the model, the primary and secondary waves can be partly trapped inside the inhomogeneities, while some part of the wave energy can escape through the boundary. From the model we obtain that the threshold and the saturation level of the wave amplitudes depends on this rate of energy escape and the scale of the inhomogeneity. For the case relevant to our observations the wave amplitude depends on the inhomogeneity scale as $|\vec{E}_0| \sim 1/L$. This result was compared with the statistics of the observations of electrostatic wave amplitudes and modulation scales provided by WBD instrument of Cluster and the observations were shown to be consistent with the predicted dependence. The major restrictive factor in this analysis was the limited length of the waveform
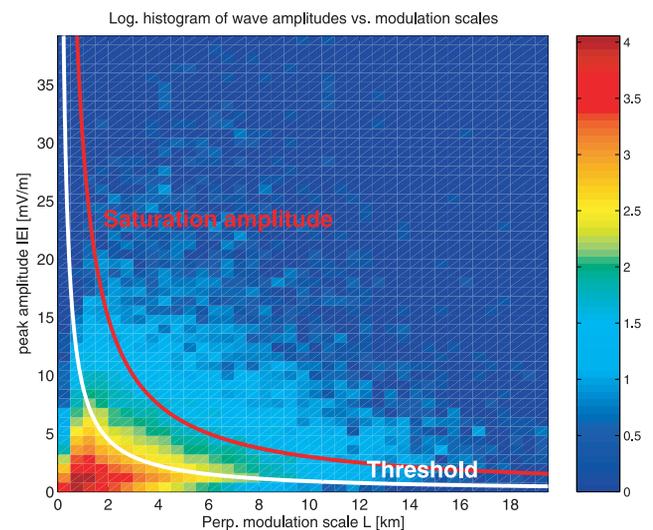
sound wave and an ion-sound wave. The instability thresholds for both decay processes can be written in the form (1), if the damping rate, frequency, and wave number of the corresponding wave modes are substituted. In homogeneous plasma the threshold of the Langmuir → Langmuir decay is comparable or even lower than the one of the Langmuir → electron-sound process because the damping rate of Langmuir waves is usually several times smaller than that of electron-sound waves. We have shown, however, that spectra consistent with the decay process were observed by Cluster in the foreshock and in many cases the magnitude of the Doppler shift of the secondary waves indicates that the primary Langmuir wave decays into an electron-sound wave and an ion-sound wave. This raises the question of why or under which conditions the electron-sound form of the decay prevails.

[39] In this paper we put forward the significant influence of density and beam inhomogeneities on the development of

Figure 3. A joint two-dimensional histogram of peak wave amplitudes and characteristic modulation times converted to perpendicular spatial scales using formula (15). Color scale is logarithmic. Superimposed on the picture are curves of the threshold amplitude (equation (8)) shown by a white line and the amplitude of wave growth saturation (equation (14)) shown by a red line. All values were calculated using a value of $\theta = 15°$.

snapshot, which does not allow us to observe the whole wave packet and its size has to be extrapolated from its inner structure. Future satellite experiments may provide the opportunity to overcome this limitation and measure the packet length directly.

Appendix A:　Parametric Instability in Two Temperature Plasma

[41] In this appendix is briefly presented a theory of electrostatic waves in two-temperature plasma and their nonlinear interaction. The theory is then applied to derive equations (2)–(4) presented in the article.

[42] We consider a two-component plasma consisting of cold and hot electron populations denoted by indices c and h. The Langmuir wave dynamics is described by the first equation from the set of Zakharov equations [*Zakharov*, 1972], where the effects of low-frequency density perturbations on the high-frequency waves enter through the nonlinear term. Concerning this equation, the only significant difference for the case of two temperature plasma is the modification of Langmuir dispersion relation [*Buti and Yu*, 1981] to

$$\omega = \omega_p \left(1 + \frac{3}{2} k^2 \frac{n_{c0} T_c + n_{h0} T_h}{m n_0 \omega_p^2} \right).$$

Here n_{c0}, n_{h0}, T_c, T_h are the densities and temperatures of the cold and hot populations, respectively, $n_0 = n_{c0} + n_{h0}$ and $\omega_p^2 = n_0 e^2 / \epsilon_0 m$.

[43] The most important difference between two temperature plasmas and Maxwellian plasmas is the existence of the electron-sound wave mode, with a dispersion relation (6). The phase velocity of this mode v_{ph} satisfies the condition $v_c \ll v_{ph} \ll v_h$, where v_c and v_h are the hot and cold thermal velocities. The principal difference from the Langmuir waves is that the hot electrons can be rapidly redistributed to satisfy the quasi-neutrality condition, while the cold population behaves more like a fluid. In this sense, the electron-sound waves are similar to ion-sound waves, except the cold electrons play the role of ions. In the following text, we derive an equation describing the nonlinear behavior of these waves in a similar way as Zakharov equations.

[44] Let us consider the high-frequency and low-frequency plasma perturbations separately. This approach will result in the following representation of density perturbations for the cold and hot components:

$$n_c = n_{c0} + \delta n_{es} + \delta n_s$$

$$n_h = n_{h0} + \delta n_{hes} + \delta n_{hs}$$

$$N = n_{c0} + n_{h0} + \delta n_s + \delta n_{hs}.$$

Here δn_{es} and δn_s are the density perturbations of cold electron population corresponding to high-frequency electron-sound wave and low-frequency ion-sound fluctuations, respectively. Similarly, δn_{hes} and δn_{hs} are the hot component perturbations and N is the ion-density obtained from quasi-neutrality condition. In the hydrodynamic approximation,

the high-frequency fluctuations of the cold plasma electrons can be described by the following equations:

$$\frac{\partial \, \delta n_{es}}{\partial t} + \text{div}[(n_{c0} + \delta n_s) \vec{v}] = 0 \tag{A1}$$

$$\frac{\partial \vec{v}}{\partial t} = \frac{e}{m} \nabla \phi_{es} - \frac{3 k_B T_c}{m n_{c0}} \nabla \, \delta n_{es}. \tag{A2}$$

Here $\vec{v}$ is the bulk velocity of the high-frequency motion of the cold electron population and ϕ_{es} is the electrostatic potential corresponding to the electrostatic waves. We keep only the most important nonlinear term introducing the low-frequency density perturbations to the high-frequency equation, analogically with the Zakharov equation. The hot population is distributed in the electrostatic potential and, taking into account that its density is small with respect to the density of cold component $n_{h0} \ll n_{c0}$, we can keep only the terms linear in the perturbations:

$$\delta n_{hes} = n_{h0} \exp\left(\frac{e\phi_{es}}{k_B T_h} \right) - n_{h0} \approx n_{h0} \frac{e\phi_{es}}{k_B T_h}. \tag{A3}$$

Substituting this into the Poisson equation, we get

$$\Delta \phi_{es} = \frac{e}{\epsilon_0} (\delta n_{es} + \delta n_{hes}) = \frac{e \, \delta n_{es}}{\epsilon_0} + \frac{n_{h0} e^2 \phi_{es}}{\epsilon_0 k_B T_h}. \tag{A4}$$

and from equations (A1)–(A3) now follows

$$\frac{\partial^2}{\partial t^2} \left(\Delta \phi_{es} - \frac{1}{\Lambda_{Dh}^2} \phi_{es} \right) + \omega_{pc}^2 \left(1 + \frac{3 T_c}{T_h} \frac{n_{h0}}{n_{c0}} \right) \Delta \phi_{es} - \frac{3 k_B T_c}{m} \Delta^2 \phi_{es}$$

$$= -\omega_{pc}^2 \left(1 + \frac{3 T_c}{T_h} \frac{n_{h0}}{n_{c0}} \right) \text{div} \left[\frac{n_S}{n_{c0}} \nabla \phi_{es} \right], \tag{A5}$$

where Λ_{Dh} and ω_{pc} are defined in section 3. Similar equation was obtained by *Schriver et al.* [2000] using slightly different approximations. To describe the interaction of the primary Langmuir wave with the electron sound wave, one should replace in the nonlinear term on the right-hand side of the equation the electrostatic potential of electron-sound wave ϕ_{es} by electrostatic potential of the Langmuir wave ϕ_L.

[45] To describe the low-frequency dynamics of plasma, we assume that electron response to the low-frequency perturbations corresponds to Boltzmann equilibrium in the electrostatic field of the two potentials: the potential of low-frequency wave ϕ_s and the ponderomotive potential originating from the modulated Langmuir and electron-sound waves [*Hanssen et al.*, 1994]:

$$\frac{\delta n_s}{n_{c0}} = \exp\left(\frac{e\phi_s}{k_B T_c} - \frac{\omega_p^2 \epsilon_0 \, (\nabla \phi_{es}, \nabla \phi_L)}{k_B T_c n_0 \omega_L \omega_{es}} \right) - 1$$

$$\approx \frac{e\phi_s}{k_B T_c} - \frac{\omega_p^2 \epsilon_0 \, (\nabla \phi_{es}, \nabla \phi_L)}{k_B T_c n_0 \omega_L \omega_{es}} \tag{A6}$$

$$\frac{\delta n_{hs}}{n_{h0}} = \exp\left(\frac{e\phi_s}{k_B T_h} - \frac{\omega_p^2 \epsilon_0 \, (\nabla \phi_{es}, \nabla \phi_L)}{k_B T_h n_0 \omega_L \omega_{es}} \right) - 1$$

$$\approx \frac{e\phi_s}{k_B T_h} - \frac{\omega_p^2 \epsilon_0 \, (\nabla \phi_{es}, \nabla \phi_L)}{k_B T_h n_0 \omega_L \omega_{es}}. \tag{A7}$$

The ion dynamics at the low frequencies can be described in hydrodynamic approximation by linear equations of similar form as (A1)–(A2) that can be combined into

$$\frac{\partial^2 \delta N}{\partial t^2} - \frac{n_0 e}{M_i}\Delta\Psi_S - \frac{5/3 k_B T_i}{M_i n_0}\Delta\,\delta N = 0, \qquad (A8)$$

where we introduced the total ion density perturbation δN. Taking into account the quasi-neutrality condition $\delta N = \delta n_s + \delta n_{hs}$, we get

$$\delta N = \left(\frac{n_{c0}}{k_B T_c} + \frac{n_{h0}}{k_B T_h}\right)\left(e\phi_s - \frac{\omega_p^2 \epsilon_0 (\nabla\phi_{es}, \nabla\phi_L)}{n_0 \omega_L \omega_{es}}\right)$$

and after simplification

$$e\Psi_s = \frac{\omega_p^2 \epsilon_0 (\nabla\phi_{es}, \nabla\phi_L)}{n_0 \omega\omega_{es}} + \frac{k_B T_c T_h}{n_{c0} T_h + n_{h0} T_c}\delta N.$$

This results in the following equation for ion density perturbations:

$$\frac{\partial^2 \delta N}{\partial t^2} - C_s^2\Delta\,\delta N = -\frac{\omega_p^2 \epsilon_0}{M_i \omega_L \omega_{es}}\Delta(\nabla\phi_L, \nabla\phi_{es}), \qquad (A9)$$

where the modified ion-sound speed C_s is defined in section 3.

[46] To obtain the equations describing the parametric instability, we assume the resonant conditions (5) to be satisfied and for each wave we decompose the space and time variations of density and field potentials into fast harmonic oscillations and a slow modulation component:

$$\phi_L = \Psi_L(\vec{r}, t)\exp\left(-i\omega_L t + i\vec{k}_L\vec{r}\right)$$
$$\phi_{es} = \Psi_{es}(\vec{r}, t)\exp\left(-i\omega_{es}t + i\vec{k}_{es}\vec{r}\right) \qquad (A10)$$
$$\delta N = \rho_s(\vec{r}, t)\exp\left(-i\omega_s t + i\vec{k}_s\vec{r}\right).$$

The factors in front of the exponentials in the above equations represent the wave modulation that is considered to be slow with respect to the wave oscillations in the sense

$$\omega_L\Psi_L \gg \frac{\partial\Psi_L}{\partial t}\ ,\ \ \left|\vec{k}\right|\Psi_L \gg |\nabla\Psi_L| \qquad (A11)$$

for Langmuir wave potential and similarly for the other quantities. Now we substitute the above representation into equations (A5), (A9), and the ordinary Zakharov equation for Langmuir waves, use relations (A11) to eliminate negligible terms and replace the second time derivatives with

$$\frac{\partial^2}{\partial t^2} \equiv -\omega^2 - 2i\omega\frac{\partial}{\partial t}$$

to get

$$\left(\frac{\partial}{\partial t} + \vec{v}_{ges}\nabla\right)\Psi_{es} = -i\frac{\omega_{pc}^2\left(\vec{k}_{es}, \vec{k}_L\right)}{2\omega_{es}\left(k_{es}^2 + \Lambda_{Dh}^{-2}\right)}\left(1 + \frac{3 T_c}{T_h}\frac{n_{h0}}{n_{c0}}\right)\frac{\rho_s^*}{n_{c0}}\Psi_L.$$

[47] Taking into consideration that $k_{es}^2\Lambda_{Dh}^2 \gg 1$ and $\frac{3 T_c}{T_h}\frac{n_{h0}}{n_{c0}} \ll 1$, we obtain the equation (3) presented in the text:

$$\left(\frac{\partial}{\partial t} + \vec{v}_{ges}\nabla\right)\Psi_{es} = -i\frac{\omega_{pc}^2\left(\vec{k}_{es}, \vec{k}_L\right)}{2 n_{c0}\omega_{es}k_{es}^2}\rho_s^*\Psi_L.$$

[48] Applying similar approximations to the other equations, one gets equation (2) for Langmuir waves and equation (4) for ion-sound waves. Note that in the main text, we used index 0 to denote the primary Langmuir decay, which exactly corresponds to index L used throughout the appendix.

References

Alekhin, J. K., et al. (1971), On the stability of an electron beam injected along geomagnetic field, *Cosmic Electrodyn.*, *2*, 280–292.

Alterkop, B. A., A. S. Volokitin, and V. P. Tarakanov (1976), The nonlinear stage of parametric interaction between waves in an active media, *Sov. Phys. JETP*, *44*, 287–291.

Anderson, R. R., et al. (1981), Plasma waves associated with energetic particles streaming into the solar wind from the earth's bow shock, *J. Geophys. Res.*, *86*, 4493–4510.

Bale, S. D., D. Burgess, P. J. Kellogg, K. Goetz, and S. J. Monson (1997), On the amplitude of intense langmuir waves in the terrestrial electron foreshock, *J. Geophys. Res.*, *102*, 11,281–11,286.

Bale, S. D., P. J. Kellogg, K. Goetz, and S. J. Monson (1998), Transverse z-mode waves in the terrestrial electron foreshock, *Geophys. Res. Lett.*, *25*, 9–12.

Bale, S. D., D. E. Larson, R. P. Lin, P. J. Kellogg, K. Goetz, and S. J. Monson (2000), On the beam speed and wavenumber of intense electron plasma waves near the foreshock edge, *J. Geophys. Res.*, *105*, 27,353–27,367.

Baumjohann, W., and R. Treumann (1996), *Basic Space Plasma Physics*, Imperial College Press, London.

Bers, A. (1984), Space-time evolution of plasma instabilities - absolute and convective, in *Handbook of Plasma Physics*, vol. 1, edited by R. Z. Sagdeev and M. Rosenbluth, pp. 451–518, North Holland, New York.

Buti, B., and M. Y. Yu (1981), Langmuir solitons in two-temperature plasma, *J. Plasma Phys.*, *26*(2), 309–316.

Cairns, I. H., and P. A. Robinson (1992), Theory for low-frequency modulated Langmuir wave packets, *Geophys. Res. Lett.*, *19*, 2187–2190.

Celnikier, L. M., L. Muschietti, and M. V. Goldman (1987), Aspects of interplanetary plasma turbulence, *Astron. Astrophys.*, *181*, 138–154.

Drummond, W. E., and D. Pines (1962), *Nucl. Fusion Suppl.*, *3*, 1049–1057.

Feldman, W. C., J. R. Asbridge, S. J. Bame, M. D. Montgomery, and S. P. Gary (1975), Solar wind electrons, *J. Geophys. Res.*, *80*, 4181–4196.

Gorbunov, L. (1977), On the theory of absolute parametric instabilities, *Sov. Phys. Tech. Phys.*, *47*(1), 36–45.

Gurnett, D. A., et al. (1997), The wide-band plasma wave investigation, *Space Sci. Rev.*, *79*, 195–208.

Hanssen, A., H. Pecseli, L. Steflo, and J. Trulsen (1994), Nonlinear wave interactions in two-electron-temperature plasmas, *J. Plasma Phys.*, *51*(3), 423–432.

Hughes, D. W., and M. R. Proctor (1990), Chaos and nois in three wave mode coupling, *Physica D*, *46*, 163–176.

Johnstone, A. D., et al. (1997), Peace: a plasma electron and current experiment, *Space Sci. Rev.*, *79*, 351–398.

Kellogg, P. J., et al. (1996), Early wind observations of bow shock and foreshock waves, *Geophys. Res. Lett.*, *23*, 1243–1246.

Kellogg, P. J., K. Goetz, S. J. Monson, and S. D. Bale (1999), Langmuir waves in a fluctuating solar wind, *J. Geophys. Res.*, *104*(13), 17,069–17,078.

Laval, G., R. Pellat, and D. Pesme (1976), Absolute parametric excitation by an imperfect pump or by turbulence in an inhomogeneous plasma, *Phys. Rev. Lett.*, *36*, 192–196.

Le Queau, D., R. Pellat, and A. Saint-Mark (1981), Electrostatic instabilities of a finite electron beam propagating in cold magnetized plasma, *Phys. Rev. A*, *24*, 448–467.

Lefebvre, B. (2000), Propriétés dynamiques et statistiques d'un petit ensemble d'ondes en interaction, Ph.D. thesis, Univ. of Orléans, Orléans, France.

Maksimovic, M., S. P. Gary, and R. M. Skoug (2000), Solar wind electron suprathermal strength and temperature gradients: Ulysses observations, *J. Geophys. Res.*, *105*, 18,337–18,350.

Matsiborko, N., et al. (1972), On nonlinear theory of instability of a monoenergetic beam in plasma, *Plasma Phys.*, *14*, 591–600.

Mikhailovskii, A. B. (1974), *Theory of Plasma Instabilities*, vol. 1, Consult. Bur., New York.

Musher, S. L., A. M. Rubenchik, and V. E. Zakharov (1995), Weak langmuir turbulence, *Phys. Rep.*, *252*, 177–274.

Percival, D. B., and A. T. Walden (1993), *Spectral Analysis for Physical Applications*, Cambridge Univ. Press, New York.

Pesme, D., G. Laval, and R. Pellat (1973), Parametric instabilities in bounded plasmas, *Phys. Rev. Lett.*, *31*, 203–206.

Robinson, P. A., and I. H. Cairns (1995), Maximum langmuir fields in planetary foreshocks determined from the electrostatic decay threshold, *Geophys. Res. Lett.*, *22*, 2657–2660.

Romanov, Y. A., and G. F. Filippov (1961), Interaction of fast electron beams with longitudinal plasma waves, *Sov. Phys. JETP*, *13*, 87–96.

Schriver, D., M. Ashour-Abdalla, V. Sotnikov, P. Hellinger, V. Fiala, R. Bingham, and A. Mangeney (2000), Excitation of electron acoustic waves near the electron plasma frequency and at twice the plasma frequency, *J. Geophys. Res.*, *105*, 12,919–12,928.

Shapiro, V. D. (1963), Nonlinear theory of oscillations excited by the interaction of a monoenergetic beam of charged particles with a plasma, *Sov. Phys. JETP*, *17*, 416–426.

Shapiro, V. D., and R. Z. Sagdeev (1997), Nonlinear wave-particle interaction and conditions for the applicability of quasilinear theory, *Phys. Rep.*, *283*, 49–71.

Sigsbee, K., C. A. Kletzing, D. A. Gurnett, J. S. Pickett, A. Balogh, and E. Lucek (2004), The dependence of Langmuir wave amplitudes on position in Earth's foreshock, *Geophys. Res. Lett.*, *31*, L07805, doi:10.1029/2004GL019413.

Vedenov, A. A., E. P. Velikhov, and R. Z. Sagdeev (1961), Nonlinear oscillations in rarefied plasma (in Russian), *Nucl. Fusion*, *1*(2), 82–100.

Vyshkind, S. Y., and M. I. Rabinovich (1976), The phase stochastization mechanism and the structure of wave trubulence in dissipative media, *Sov. Phys. JETP*, *44*, 292–299.

Zakharov, V. E. (1972), Collapse of langmuir waves, *Sov. Phys. JETP*, *35*(5), 908–914.

————————————

T. Dudok de Wit and V. Krasnoselskikh, Laboratoire de Physique and Chimie de l'Environement, CNRS, 3A, Av. de la Recherche Scientifique, 45071 Orléans, France.

C. A. Kletzing and J. S. Pickett, Department of Physics and Astronomy, University of Iowa, Iowa City, IA 52242, USA.

J. Soucek, Department of Space Physics, Institute of Atmospheric Physics, Boční II/1401, 14131 Prague 4, Czech Republic. (soucek@ufa.cas.cz)